Sm³⁺ ions doped zinc barium tellurite oxyfluoride glasses for laser materials

Yaowalak YAMSUK[1,2], Patarawagee YASAKA[1,2], Jakrapong KAEWKHAO[1,2], and Narong SANGWARANATEE[3,*]

[1] *Physics Program, Faculty of Science and Technology, Nakhon Pathom Rajabhat University, 73000, Thailand*
[2] *Center of Excellence in Glass Technology and Materials Science (CEGM), Nakhon Pathom Rajabhat University, Nakhon Pathom 73000, Thailand*
[3] *Applied Physics, Faculty of Science and Technology, Suan Sunandha Rajabhat University, Bangkok 10300, Thailand*

*Corresponding author e-mail: narong.sa@ssru.ac.th

Abstract

The Sm³⁺ ions were doped tellurite glasses with composition (55-x) TeO_2-10ZnF_2-35BaO-xSm_2O_3 (where x = 0.00, 0.05, 0.10, 0.50, 1.00 and 1.50 in mol%) to investigate the physical, the optical, the luminescence and structural properties. The functional groups can be identified using FT-IR spectra of Sm³⁺ in the glasses. The most intense peak from emission spectra is at 600 nm ($^4G_{5/2}{\rightarrow}^6H_{7/2}$) corresponding to reddish-orange color. The oscillator strengths were resolved from the absorption spectra and then used to calculate the Judd–Ofelt (J–O) intensity parameters. The radiative properties were calculated by J–O intensity parameters for various transitions in tellurite glass matrices. According to the results of stimulated emission cross section, lifetime and the branching ratio of the emission transition $^4G_{5/2}{\rightarrow}^6H_{7/2}$, it is promised that 0.50 mol% of Sm_2O_3 doped tellurite glasses is the potential laser material.

1. Introduction

Rare earth (RE) doped glasses have been studied especially in optical practices for several applications such as display monitor, optical detectors, optical fibres, sensors and solid state lasers [1-4]. One of rare earth ions popularly doped in glasses is Sm³⁺. That exhibited peak and highest emission peak in the range of 550-700 nm, are suitable for using Sm³⁺ ion as the dopant for orange or orange-red emission [5]. The glasses doped with them emit reddish orange light by reason of the $^4G_{5/2} \rightarrow {}^6H_J$ (J = 5/2, 7/2, 9/2, 11/2) transitions. Thus, they are suitable for applications integrated in powerful lasers, display devices, submarine communication and high dense information storage devices [6,7]. Tellurite based glasses have the remarkable properties such as low phonon energy (700-800 cm⁻¹), high refractive index (1.9-2.4), relatively low melting temperature (about 800°C) and moisture resistant [8-10]. Their low phonon energy reduced the non-radiative transitions from excited states to lower energy levels of rare earth ions, therefore the luminescence intensity is increased. The obvious nonlinear optical properties of TeO_2 based glasses emerged by the high hyper polarity of electron pair related with the 5s orbital of the tellurium atom [11]. However, in the field of optics, nonlinear effects became a subject of interest only after the invention of the laser. After the invention of laser, many classical experiments in Nonlinear Optical (NLO) such as experiments on Second Harmonic Generation (SHG) by Franken et al, in 1961, Sum Frequency Generation

(SFG) by Bass et al in 1962 and optical rectification by Bass et al in 1962 were performed. Since then, NLO had become a rapidly growing field in Physics. Nonlinearities are found everywhere in optical applications and at present, nonlinear optical properties of many optical materials with significant relevance to technological and optical applications have been found [12]. The glass structure has weaker Te-O bonds which can be simply broken and helpful for taking rare earth ions and other heavy metal oxides [13]. In this work, the tellurite glasses doped with varied concentrations of Sm³⁺ions were prepared. Accordingly, their physical and spectroscopic properties were measured and analyzed. The Judd-Ofelt intensity parameters were also computed using the absorption data of the glass samples. The computations were particularly operated for different Sm_2O_3 concentration. The emission properties of glass samples for different Sm_2O_3 concentration were also discussed in particulars.

2. Experimental

2.1 Glass preparation

The glass samples were prepared with composition (55-x)TeO_2-10ZnF_2-35BaO-xSm_2O_3 (where x = 0.00, 0.05, 0.10, 0.50, 1.00 and 1.50 in mol%) using a normal melt quenching technique. The raw materials were mixed into 6 batches each of 15 g. The mixtures were homogeneous by crushing in an agate mortar and then put into a porcelain crucible. The containers were

put into electrical furnace operated at 950°C for 1 h for the mixtures to be melted. Each batch of melting materials was poured into the preheated graphite plate and then coupled by another graphite plate to undergo uniform thickness. Then, they were annealed in an furnace for 3 h at 350°C to eliminate strain, adjust the mechanical strength, and left to reach the room temperature. The samples then were cut and adipose to the dimension of $1.0 \times 1.5 \times 0.3$ cm³ for further optical measurements.

2.2 Physical and optical studies

The Sm^{3+} doped tellurite glass samples were brought to measure their density via Archimedes method using the densitometer HR-200 weighing balance. The refractive index of these samples were measured at room temperature by using Reflectivity Meter (PRM). The physical properties: density, molar volume, refractive index of the samples with various concentration of Sm^{3+} ions are summarized in Table 1. Fourier transform infra-red (FTIR) spectra of the glasses were obtained by a Agilent Technologies Cary 630 FTIR system with a spectral resolution of 4 cm⁻¹ [14]. The optical absorption spectra were investigated in the UV-Vis-NIR range corresponding to 200-2,500 nm using a UV–3600 Shimadzu UV–VIS–NIR spectrophotometer. The Cary Eclipse Fluorescence Spectrophotometer was used to examine the excitation and emission spectra of the samples. The instrument was also operated to measure the lifetimes of the transition from the $^{4}G_{5/2}$ excited level of Sm^{3+} ion under the 404 nm incident light. The J-O intensity parameters which accord significant information regarding local structure and bonding in the neighbourhood of Sm^{3+} ion have been computed and reported.

3. Results and discussion

3.1 Physical properties

Figure 1 displays the density (ρ) and molar volume (V_M) on the concentration of Sm_2O_3. The fluctuating density of glasses are not depended on Sm_2O_3

concentration. The molar volumes of glasses tent to increase with increasing of Sm_2O_3 concentration, reflecting that the glass structure was expanded with higher concentration of Sm_2O_3. Higher ionic radius values of Sm^{3+} ions result in increased value of the molar volume. [15,16], reflecting that more non-bridging oxygen has been increased. The density (ρ) are between 5.27 ± 0.005 to 5.34 ± 0.109 g·cm⁻³ while their molar volumes (V_M) are between 28.39 to 30.32 cm³·mol⁻¹. Refractive index were increased with density value, which it is general trend for optical material.
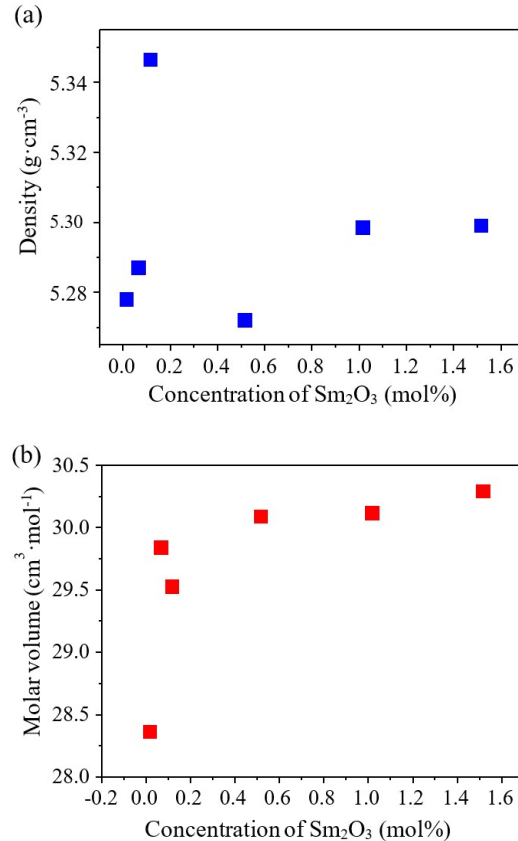

Figure 1. (a) Density (ρ) and (b) molar volume (V_M) of tellurite glasses doped with Sm^{3+}.

Table 1. Physical properties of the Sm^{3+} ion doped zinc-barium-borate glasses.

Sample No.	Physical properties	0.00 mol%	0.05 mol%	0.10 mol%	0.50 mol%	1.00 mol%	1.50 mol%
1	Density (g·cm⁻³)	5.27± 0.002	5.28± 0.012	5.34± 0.006	5.27± 0.001	5.29± 0.004	5.30± 0.006
2	Molar Volume (cm³·mol⁻¹)	28.39	29.87	29.55	30.11	30.14	30.32
3	Refractive index	1.60	1.83	1.85	1.86	1.87	1.87

3.2 FTIR spectra analysis

This technique establishes exploring of structural systems related to both local structures in the glasses matrix and the anionic places with the modifying cation [17]. The spectra were measured in the wavenumber range of 650-4,000 cm^{-1}. The vibrational spectra of the Sm_2O_3 are appear in Figure 2., the band positions together with their assignments are displays in Table 2. [18-20] It was observed that as the Sm_2O_3 concentration increases the intensity of OH band decreases, this indicates that Sm^{3+} doped tellurite glasses are suitable for high grade optical glasses with low OH content. [21] The peaks at 816-839 cm^{-1} can be assigned to the symmetric stretching bending vibrations of the Te-O-Te linkages of $[TeO_3]$ structural units. [22] The shoulder around 1057-1082 cm^{-1} may be designated to the Stretching vibrations of Te–NBO [23]. The band around 2138-2176 cm^{-1} is due to stretching vibration of OH group and bands around 2963-2989 cm^{-1} are due to OH group. [24]
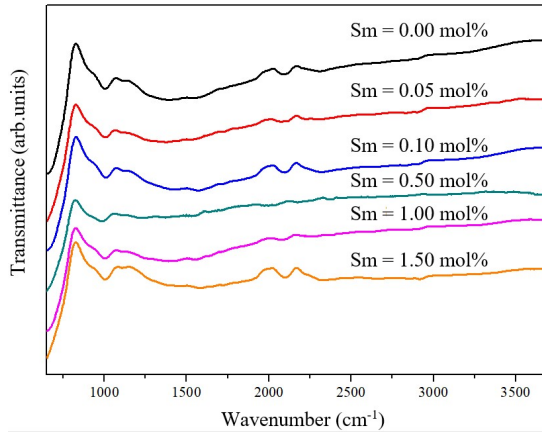
Figure 2. FTIR spectra of Sm^{3+} ion doped tellurite glasses.

3.3 Absorption spectra

UV-VIS-NIR absorption spectra of Sm_2O_3 doped tellurite glasses are presented in Figure 3. The optical spectra of glass represent seven absorption bands at 948, 1086, 1249, 1395, 1505 and 1553 nm which are due to the Sm^{3+} transitions from $^6H_{5/2}$ to $^6F_{11/2}$, $^6F_{9/2}$, $^6F_{7/2}$, $^6F_{5/2}$, $^6F_{3/2}$ and $^6H_{15/2}$ serially. Furthermore, the absorption increased with increasing of Sm_2O_3

concentration. These results show higher absorption potentiality of tellurite glass with more quantity of Sm^{3+} in glass.
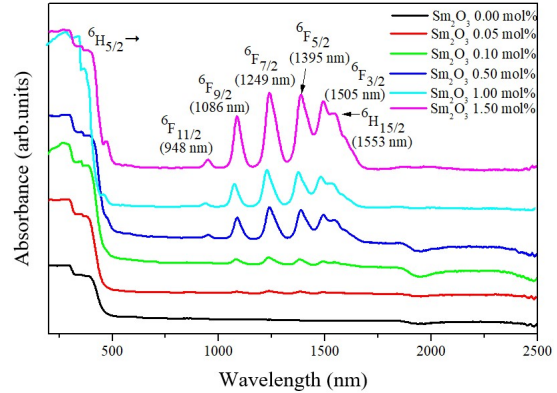
Figure 3. The absorption spectra of tellurite glasses doped with Sm^{3+} ions.

3.4 Judd–Ofelt intensity parameters

Judd-Ofelt theory is important for calculating the differentiation intensity of the rare earth ions in several host matrices [25,26]. The J-O parameters were used to analyze the various radiative properties of Sm^{3+} ion for example radiation transition probability, branching ratio, radiative lifetime and stimulated emission cross-section (σ_{rms}). The approximation of the calculated oscillator strength (f_{cal}) of an electric dipole transition was done for Sm^{3+} ion within the 4f shell using the equation

$$f_{cal} = \left[\frac{8\pi^2 mcv}{3h(2J+1)} \right] \left[\frac{(n^2+2)^2}{9n} \right] \times \sum_{\lambda=2,4,6} \Omega_\lambda (\psi J \| U^\lambda \| \psi 'J')^2 \quad (1)$$

Where m is the electron mass; J is the angular momentum (kg m^2·s^{-2}), v is the energy of the transition in cm^{-1}, Ω_λ (λ = 2, 4 and 6) are the JO intensity parameters and $\| \psi^\lambda \|^2$ are the doubly reduced matrix elements of the unit tensor operator [27] c is the light speed, n is the refractive index, h is Planck's constant and $\| \psi^\lambda \|^2$ are the doubly reduced square matrix elements of the unit tensor operator which are evaluated from the intermediate coupling approximation for a transition from ψJ to ψ 'J' state [28]. $<\| U^\lambda \|>$ is independent of the host matrix.

Table 2. FTIR band positions (cm^{-1}) and their peak assignments of tellurite glasses.

Sample No.	0.00 mol%	0.05 mol%	0.10 mol%	0.50 mol%	1.00 mol%	1.50 mol%	Assignments
1	830	822	829	817	816	839	Symmetricstretching bending of Te-O bonds
2	1057	1073	1075	1067	1082	1067	Stretching vibrations of Te-NBO
3	2173	2174	2176	2138	2166	2169	O-H group stretching vibrations
4	2963	2979	2989	2966	2981	2984	OH group

$(n^2 + 2)^2 /9n$ is the Lorentz local field correction factor which indicates that the ions are calculated in a dielectric medium but not in a vacuum [29]. The experimental oscillator strength (f_{exp}) were calculated by integrating area under each absorption bands of the Sm^{3+} ion doped tellurite glasses using the equation.

$$f_{exp} = 4.318 \times 10^{-9} \int \varepsilon(v)dv \qquad (2)$$

Where $\varepsilon(v)$ is the molar extinction coefficient at v energy cm^{-1}. The JO theory [30,31] gives the oscillator strength, f, of a transition from the ground state to an excited state. If the transition is of electric dipole type, the calculated oscillator strength from the ground state to an excited state is given. The equation use to calculate the root mean square deviation (rms), σ^{rms}, between (f_{exp}) and (f_{cal}) follow as

$$\sigma_{rms} = \left[\frac{\sum (f_{exp} - f_{cal})^2}{N} \right]^{1/2} \qquad (3)$$

Where N is number of levels included in the fit. The total emission cross-sections of Sm^{3+} doped tellurite glasses are shown in Table. 3. The results show the complementary between the experimental results and calculated oscillator strengths [32]. The values of the f_{cal} and f_{exp} were calculated by equation 1 and 2 respectively and the results are show in Table 4 for different Sm^{3+} ions content. The JO intensity parameters are host dependent and are important inexploring the glass structure and transition rate of the rare earth ion energy levels. The trends of the JO parameters are found to be in the order of $\Omega_4 > \Omega_2 > \Omega_6$ for the prepared Sm^{3+}: tellurite glasses. The Ω_2, JO intensity parameter of the Sm^{3+} doped glasses are found to be associated with the covalence, structural change and symmetry of the ligand field around Sm^{3+} site [33] The JO intensity parameters Ω_4 and Ω_6 refer to the viscosity of the glass matrix and dielectric of the media, which are affected by the vibronic transitions of the RE ions bound to the ligand atoms [34,35]. The structure of tellurite glasses consists of randomly connected Te-O bonds and O–H bond stretching vibrations. The observed trend in the variation of the J-O parameter was $\Omega_4 > \Omega_2 > \Omega_6$. The spectroscopic quality factors for the 0.5 mol % exist Sm_2O_3 glasses shown to be better parallel to the different glasses in the prepared series. The J-O intensity comparison between another works and $10TeO_2 - 15CaO - 5ZnO - 10Nb_2O_5 - 59B_2O_3 - Sm_2O_3$ are shown in Table 5.

Table 3. Experimental and calculated oscillator strengths ($\times 10^{-6}$) for 0.5 mol% and the total emission cross-section of Sm^{3+} ion doped tellurite glasses.

Transition	λ_p (nm)	σ_e ($\times 10^{-22}$ cm²)	$\beta_{(R)}$ Exp	Cal
$^4G_{5/2} \to {}^6H_{5/2}$	563	0.035	0.124	0.117
$^4G_{5/2} \to {}^6H_{7/2}$	600	0.036	0.514	0.379
$^4G_{5/2} \to {}^6H_{9/2}$	645	0.056	0.331	0.283
$^4G_{5/2} \to {}^6H_{11/2}$	707	0.024	0.030	0.079

Table 4. The absorption peak wavelength (λ, nm), energy (v, cm^{-1}), experimental (f_{exp}) and calculated (f_{cal}) oscillator strengths (10^{-6}) of Sm^{3+} 0.5 mol% doped tellurite glass along with Judd-Ofelt intensity parameters ($\Omega_{2,4,6}$, $\times 10^{-20}$ cm²) [36,37].

Transition $^5H_{5/2} \to$	λ (nm)	v (cm⁻¹)	f_{exp}	f_{cal}
$^6F_{11/2}$	948	10548	0.524	0.538
$^6F_{9/2}$	1086	9208	1.151	0.824
$^6F_{7/2}$	1249	8006	1.496	1.024
$^6F_{5/2}$	1395	7168	1.174	1.794
$^6F_{3/2}$	1505	6644	0.916	1.244
$^6F_{1/2} + {}^6H_{15/2}$	1553	6439	0.656	0.203
σ_{rms}			± 0.086	

Table 5. J–O intensity parameters of the Sm^{3+} ions doped tellurite glasses and other reported Sm^{3+} doped glasses.

Glass sample	J–O intensity parameters ($\times 10^{-20}$ cm²) Ω_2	Ω_4	Ω_6	Tends	Ref.
0.5mol% Sm_2O_3	1.33	1.40	1.14	$\Omega_4 > \Omega_2 > \Omega_6$	Present work
PTBEu01	2.77	5.22	0	$\Omega_4 > \Omega_2 > \Omega_6$	[38]
TSWS10	0.070	3.048	2.706	$\Omega_4 > \Omega_6 > \Omega_2$	[39]
ZLiBiB: Sm^{3+}	2.03	1.92	1.88	$\Omega_2 > \Omega_4 > \Omega_6$	[40]
Sm^{3+}:SFB	3.51	3.48	4.56	$\Omega_6 > \Omega_2 > \Omega_4$	[41]

3.5 Excitation and emission studies

Figure 4. The excitation spectra (λ_{em} = 600 nm) of the Sm^{3+} ions doped tellurite glasses. The excitation spectra of tellurite glasses. The spectra display different excited peaks from the ground state to various excited states of the Sm^{3+} those obtain the emission at 600 nm. The peaks remark are pointed as $^6H_{5/2} \rightarrow ^4H_{9/2}$ (346 nm), $^6H_{5/2} \rightarrow ^4D_{3/2}$ (363 nm), $^6H_{5/2} \rightarrow ^6P_{7/2}$ (377 nm), $^6H_{5/2} \rightarrow ^4L_{15/2}$ (390 nm), $^6H_{5/2} \rightarrow ^4F_{7/2} + ^4K_{11/2}$ (404 nm), $^6H_{5/2} \rightarrow ^6P_{5/2}$, $^4P_{5/2}$ (418 nm), $^6H_{5/2} \rightarrow ^4G_{9/2}$ (439 nm), $^6H_{5/2} \rightarrow ^4I_{11/2}$ (474 nm), $^6H_{5/2} \rightarrow ^4G_{7/2}$ (500 nm) and $^6H_{5/2} \rightarrow ^4F_{3/2}$ (528 nm) [36, 37] as show in Figure 4. The highest peak of excitation spectra is observed at 404 nm.
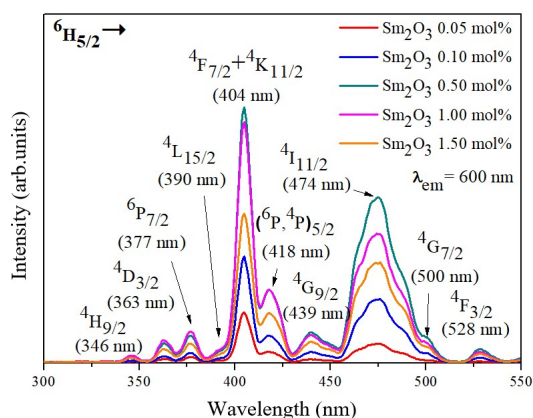

Figure 4. The excitation spectra (λ_{em} = 600 nm) of the Sm^{3+} ions doped tellurite glasses.

Figure 5 present the emission spectra of the Sm^{3+} doped tellurite glasses at an excitation wavelength of 404 nm. The spectra appear in four significant peaks together with the nominal peak at the longer wavelength. The observed emission peaks at 563 nm, 600 nm, 645 nm and 707 nm. These peaks are coincident to $^4G_{5/2} \rightarrow ^6H_{5/2}$, $^4G_{5/2} \rightarrow ^6H_{7/2}$, $^4G_{5/2} \rightarrow ^6H_{9/2}$ and $^4G_{5/2} \rightarrow ^6H_{11/2}$, the transitions of the Sm^{3+} ion. The highest peak of emission spectra is observed at 600 nm. Figure 5. shows the intensity variation for the $^4G_{5/2} \rightarrow ^6H_{7/2}$ transition from this figure it is clear that emission intensity increased up to 0.50 mol % and then it decreased. This behavior directly related to the concentration quenching due to an increase number of Sm^{3+} ions in the glass matrix. Also as an inset is a photograph of the light output from the glass while excited at 404 nm. [37]

3.6 X-ray luminescence spectra

The X-ray luminescence spectra of the Sm^{3+} ions doped tellurite glasses are shown in Figure 6. The X-ray, from 50 kV and 30 mA operated source, were irradiated to glass samples. The Sm^{3+} ions doped tellurite glasses have four emission peaks at 563 nm, 600 nm, 645 nm and 707 nm, there are determined to

the transitions $^4G_{5/2} \rightarrow ^6H_{5/2}$, $^4G_{5/2} \rightarrow ^6H_{7/2}$, $^4G_{5/2} \rightarrow ^6H_{9/2}$ and $^4G_{5/2} \rightarrow ^6H_{11/2}$ [42]. The highest peak distinguished at 645 nm. In addition, It was found that the intensity of 1.0 mol% doped glasses is higher than other samples. There are the differences of the strongest emission peak and glass sample that possesses the highest emission intensity. It can be clarified that the hosting material and activator ions have different interaction mechanism with UV-Vis and X-ray excitation. UV-Vis directly excites only the electrons of Sm^{3+} ions, while X-ray excites both the electrons of Sm^{3+} ions and host. X-ray excitations in the host results to the hole-electron interaction, then the large number of secondary electrons are produced. Since these glasses have long decay time as a few milliseconds, it can be used for integration mode of scintillation such as in medical and industrial X-ray imaging systems. [43].
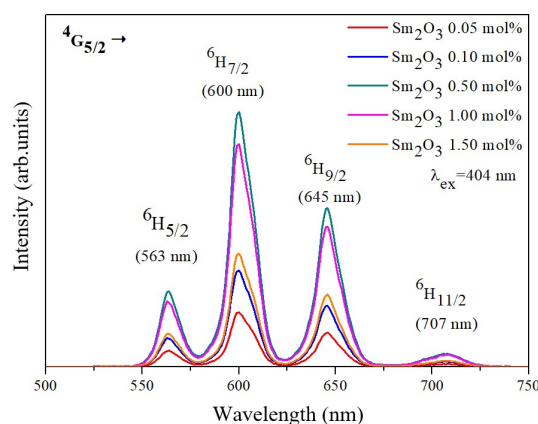

Figure 5. The mission spectra (λ_{ex} = 404 nm) of Sm^{3+} doped tellurite glasses.
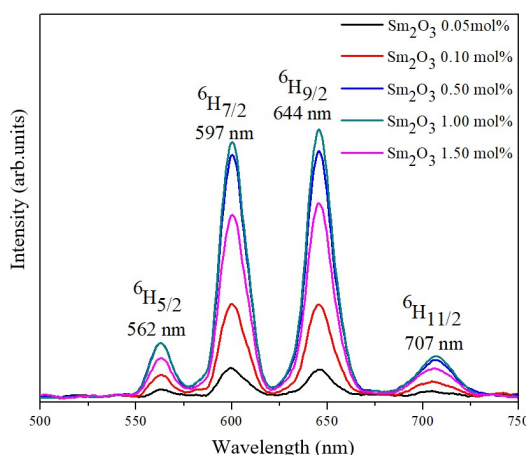

Figure 6. The x-ray luminescence spectra of the Sm^{3+} ions doped tellurite glasses.

3.7 Decay analysis

The lifetimes of the $^4G_{5/2}$ energy level for the different mol% of Sm_2O_3 were measured and the

experimental decay curves are shown in Figure 7. The increasing of the Sm^{3+} ions affect to the lifetime decreasing. This may be due to the energy transfer between excited ion and ground state ion via cross relaxation. On excitation of the Sm^{3+} ions above the $^4G_{5/2}$ level, the electrons decay to the $^4G_{5/2}$ level by fast non-radiative relaxation and emissions accordingly arise by the transition from this energy level to the lower energy levels [44].
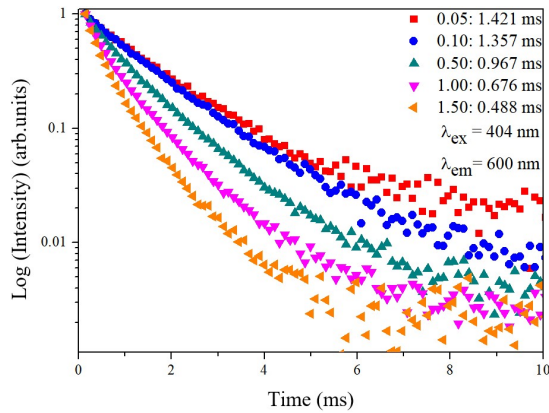

Figure 7. Florescence decay profile of the $^4G_{5/2}$ state of the Sm^{3+}ions for different concentrations doped tellurite glass.
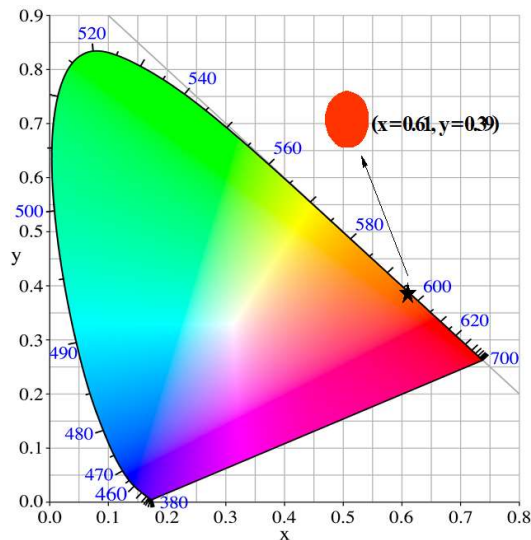

Figure 8. CIE chromaticity diagram of Sm^{3+} doped tellurite glasses.

3.8 Commission Internationale de L'Eclairage (CIE) in 1931 system

The color chromaticity of all samples were evaluated using the Commission International de L'Eclairage (CIE) 1931 system [45,46]. The hue and saturation of a color were defined while the specified emission color and color purity of a system were

indicated via its coordinates [47]. The tristimulus values $X(\lambda)$, $Y(\lambda)$ and $Z(\lambda)$ were calculated using the emission spectra together with CIE color matching functions. Accordingly, the estimation of chromaticity co-ordinates (x,y) were constructed from the tristimulus values as $x = X/(X+Y+Z)$ and $y = Y/(X+Y+Z)$. The (x,y) coordinates of the samples were found to be (0.61, 0.39) corresponding to the color marked in the CIE chromaticity diagram in Figure 8. The CIE diagram confirms that these Sm^{3+} doped tellurite glasses emit the light in reddish-orange region, which indicates its potential for use in the display applications.

4. Conclusions

The tellurite glasses doped with different Sm_2O_3 concentrations were prepared and their reddish orange emitting efficiencies were studied for the development of laser materials. The molar volumes and refractive index of glasses were increased with increasing of Sm_2O_3 concentration. The structure of tellurite glasses consists of randomly connected Te-O bonds and O–H bond. The observed trend in the variation of the J-O parameter was $\Omega_4 > \Omega_2 > \Omega_6$. The spectroscopic quality factors for the 0.5 mol % exist Sm_2O_3 glasses shown to be better parallel to the different glasses in the prepared series. The emission spectra present peaks at 563 nm, 600 nm, 645 nm and 707 nm. These peaks are corresponding to $^4G_{5/2} \rightarrow ^6H_{5/2}$, $^4G_{5/2} \rightarrow ^6H_{7/2}$, $^4G_{5/2} \rightarrow ^6H_{9/2}$ and $^4G_{5/2} \rightarrow ^6H_{11/2}$, the transitions of the Sm^{3+} ion. The X-ray luminescence spectra have peaks and transitions like the emission spectra. The lifetime values corresponding to the $^4G_{5/2}$ excited state is found to decrease with increasing in Sm^{3+} ion concentration. The CIE 1931 chromaticity co-ordinate (0.61, 0.39) are also calculated to confirm the potential of observed materials for use in optical devices. Systematic analysis of the results suggested that the glass doped with Sm_2O_3 concentration at 0.5 mol% is suitable for laser material and optical device applications.

5. Acknowledgements

References

[1]   A. Agarwal, I. Pal, S. Sanghi, and M. P. Aggarwal, "Judd–Ofelt parameters and radiative properties of Sm^{3+} ions doped zinc bismuth borate glasses," *Optical Materials*, vol. 32, no. 2, pp. 339-344, 2009

[2]   D. U. Maheswari, J. S. Kumar, T. Sasikala, A. M. Babu, K. Pavani, K. Jang, and L. R. Moorthy, "Optical absorption and fluorescence

properties of Dy³⁺: SFB glasses," in *IOP Conference Series: Materials Science and Engineering*, India, vol. 2, no. 012019, 2009.

[3] M. A. K. Elfayoumi, M. Farouk, M. G. Brik, and M. M. Elokr, "Spectroscopic studies of Sm³⁺ and Eu³⁺ co-doped lithium borate glass," *Journal of Alloys and Compounds*, vol. 492, no. 1-2, pp. 712-716, 2010.

[4] N. Chanthima, N. Kiwsakunkran, J. Kaewkhao, and N. Sangwaranatee, "Optical and luminescence investigation of Er³⁺ doped in Na₂O-Al₂O₃-P₂O₅ glasses for photonics material application," *Journal of Metals Materials and Minerals*, vol. 29, no.2, pp. 58-63, 2019.

[5] N. Luewarasirikul, J. Kaewkhao, and H. Kim, "Synthesis and luminescence properties of CaMoO4:Sm³⁺ phosphors for orange photonic materials," *Journal of Metals, Materials and Minerals*, vol. 29, no.2, pp. 64-69, 2019.

[6] S. Selvi, K. Marimuthu, G. Muralidharan, "Effect of PbO on the B₂O₃-TeO₂-P₂O₅-BaO-B₂O₃-BaO-CdO-Sm₂O₃ glasses structural and optical investigations," *Journal of Non-Crystalline Solids*, vol. 461, pp. 35-46, 2017.

[7] D. D. Ramteke, V. Y. Ganvir, S. R. Munishwar, and R. S. Gedam, "Concentration Effect of Sm³⁺ Ions on Structural and Luminescence Properties of Lithium Borate Glasses," *Physics Procedia*, vol. 76, pp. 25-30, 2015.

[8] J. S. Wang, E. M. Vogel, and E. Snitzer, "Tellurite glasses: a new candidate for fiber devices," *Optical Materials*, vol. 3, no. 3, pp. 187-203, 1994.

[9] L. Jyothi, G. Upender, R. Kuladeep, D. Narayana Rao, "Structural, thermal, optical properties and simulation of white light of titanium-tungstate-tellurite glasses doped with dysprosium," *Materials Research Bulletin*, vol. 50, pp. 424-431, 2014.

[10] I. Z. Hager, R. El-Mallawany, and A. Bulou, "Luminescence spectra and optical properties of TeO₂–WO₃–Li₂O glasses doped with Nd, Sm and Er rare earth ions," *Journal of Physics: Condensed Matter*, vol. 406, pp. 972-980, 2011.

[11] M. Udovic, P. Thomas, M. Mirgordsky, O. Durand, M. Soulis, O. Masson, T. Merle Mejean, and J. C. Champarnaud-Mesjard, "Influence of tellurite on lifetime for samarium doped lanthanum lead borate glass," *Journal of Solid State Chemistry*, 2006.

[12] J Xu, "Nonlinear Optical Materials," RW Boyd and GL Fischer, USA, 2016.

[13] A. Murali, R. Chakradhar, and J. L. Rao "EPR studies of Gd³⁺ ions in lithium tetra boro-tellurite and lithium lead tetra boro-tellurite glasses," *Physical B Condensed Matter*, vol. 364, no. 1, pp. 142-149, 2005.

[14] S. S. Sundaria, K. Marimuthuan, M. Sivramana, and S. S. Babu, "Composition dependent structural and optical properties of Sm³⁺-doped sodium borate and sodium fluoroborate glasses," *Journal of Luminescence*, vol. 130, no. 7, pp. 1313-1319, 2010.

[15] D. D. Ramteke, V. Kumar, and H. C. Swart, "Spectroscopic studies of Sm³⁺/Dy³⁺co-doped lithium boro-silicate glasses," *Journal of Non-Crystalline Solids*, vol. 438, pp. 49-58, 2016.

[16] D. D. Ramteke, H. C. Swart, and R. S. Gedam, "Spectroscopic properties of Pr³⁺ ions embedded in lithium borate glasses," *Physical B Condensed Matter*, vol. 480, pp. 111, 2016.

[17] D. Rajesh, A. Balakrishna, and Y. C. Ratnakaram, "Luminescence, structural and dielectric properties of Sm³⁺ impurities in strontium lithium bismuth borate glasses," *Optical Materials,* vol. 35, no. 2, pp. 108-116, 2012.

[18] S. Selvi, K. Marimuthu, and G. Muralidharan, "Structural and luminescence behavior of Sm³⁺ ions doped lead boro-telluro-phosphate glasses," *Journal of Luminescence*, vol. 159, pp. 207-218, 2015.

[19] E. Mansour, "FTIR spectra of pseudo-binary sodium borate glasses containing TeO₂," *Journal of Molecular Structure*, vol. 1014, pp. 1-6, 2012.

[20] A. Kaur, A. Khanna, H. Bhatt, M. Gónzález-Barriuso, F. González, B. Chen, and M. N. Deo, "B–O and Te–O speciation in bismuth tellurite and bismuth borotellurite glasses by FTIR, ¹¹B MAS-NMR and Raman spectroscopy," *Journal of Non-Crystalline Solids*, vol. 470, pp. 19-26, 2017.

[21] S. Sailaja, C. N. Raju, C. A. Reddy, D. P. R. Borelli, Y. D. Jho, and B. S. Reddy, "Optical properties of Sm³⁺ doped cadmium bismuth borate glasses," *Journal of Molecular Structure*, vol. 1038, pp. 29-34, 2013.

[22] K. Maheshvaran, P. K. Veeran, and K. Marimuthu, "Structural and optical studies on Eu³⁺ doped boro-tellurite glasses," *Solid State Sciences,* vol.17, pp. 54-62, 2013.

[23] L. Balachander, G. Ramadevudu, Md. Shareefuddin, R. Sayanna, and Y. C. Venudhar, "IR analysis of borate glasses containing three alkali oxides," *ScienceAsia*, vol. 39, pp. 278-283, 2013.

[24] C. Guatam, A. K. Yadav, and A. K. Singh, "A review on infrared spectroscopy of borate glasses with effects of different additives," *International Scholarly Research Notices*, vol. 2012, pp. 1-17, 2012.

[25] K. Maheshvaran and K. Marimuthu, "Concentration dependent Eu³⁺ doped boro-tellurite glasses Structural and optical investigations," *Journal of Luminescence*, vol. 132, no. 9, pp. 2259-2267, 2012.

[26] G. S. Ofelt, "Intensities of crystal spectra of Rare-Earth ions," *Journal of Chemical Physics*, vol. 37, pp. 511-521, 1962.

[27] C. K. Jayasankar and E. Rukmini, "Optical properties of Sm $^{3+}$ ions in zinc and alkali zinc borosulphate glasses," *Optical Materials*, vol. 8, no. 3, pp. 193-205, 1997.

[28] L. R. Moorthy, A. Radhapathy, M. Jayasimhadri, D. V. R. Moorthy, and R. V. S. S. N. R. Kumar, "Radiative emission probabilities of Dy^{3+}-doped alkali borate and fluoroborate glasses," *Journal of Alloys and Compounds*, vol. 408-412, pp. 724-727, 2006.

[29] W. T. Carnall, H. Crosswhite, and H. M. Crosswhite, *Energy level structure and transition probabilities in the spectra of the trivalent lanthanides in LaF$_3$*, 1962.

[30] B. R. Judd, "Optical Absorption Intensities of Rare-Earth Ions," *Physical Review*, vol. 127, pp. 750-761, 1962.

[31] N. Wantana, E. Kaewnuam, B. Damdee, S. Kaewjaeng, S. Kothan, H. J. Kim, and J. Kaewkhao, "Energy transfer based emission analysis of Eu^{3+} doped Gd$_2$O$_3$-CaO-SiO$_2$-B$_2$O$_3$ glasses for laser and X-rays detection material applications," *Journal of Luminescence*, vol. 194, pp. 75-81, 2018.

[32] O. Ravi, C. M. Reddy, L. Monoj, B. D. P. Raju, "Structural and optical studies of Sm^{3+} ions doped niobium borotellurite glasses," *Journal of Molecular Structure*, vol. 1029, pp. 53-59, 2012.

[33] S. Tanabe, T. Ohyagi, N. Soga, and T. Hanada, "Compositional dependence of Judd-Ofelt parameters of Er^{3+} ions in alkali-metal borate glasses," *Physical Review B Condensed matter*, vol. 46, pp.3305-3310, 1992.

[34] W. F. Krupke, "Optical absorption and fluorescence intensities in several Rare-Earth-Doped Y$_2$O$_3$ and LaF$_3$ single crystals,". *Phys.Rev*, vol. 145, pp. 325-337, 1966.

[35] G. Lakshminarayana, R. Y. M. Mao, and J. Qiu, "Spectral analysis of RE^{3+} (RE = Sm, Dy, and Tm): P$_2$O$_5$–Al$_2$O$_3$–Na$_2$O glasses," *Optical Materials*, vol. 31, no. 10, pp. 1506-1512, 2009.

[36] V. H. Rao, P. S. Prasad, M. M. Babu, P. V. Rao, L. F. Santos, G. N. Rajud, and N. Veeraiah, "Luminescence properties of Sm^{3+} ions doped heavy metal oxide telluritetungstate-antimonate glasses," *Ceramics International,* vol. 43, no. 18, pp. 16467-16473, 2017.

[37] D. D. Ramteke, A. Balakrishna, V. Kumar, and H. C. Swart, "Luminescence dynamics and investigation of Judd-Ofelt intensity parameters of Sm^{3+} ion containing glasses," *Optical Materials*, vol. 64, pp. 171-178, 2017.

[38] M. V. V. Kumar, J. B. Chinna, K. R. Gopal, and R. R. Reddy, "Novel Eu^{3+} doped lead telluroborate glasses for red laser source applications," *Journal of Solid State Chemistry,* vol. 184, no. 8, pp. 2145-2149, 2011.

[39] C. K. Jayasankar and P. Babu, "Optical properties of Sm^{3+} ions in lithium borate and lithium fluoroborate glasses," *Journal of Alloys and Compounds*, vol. 307, pp. 82-95, 2000.

[40] P. Giridhar, S. Sailaja, M. B. Reddy, K. V. Raju, C. N. Raju, and B. S. Reddy, "Spectroscopic Studies of RE^{3+} (RE = Eu, Tb, Sm & Dy): Lithium Lead Boro Tellurite Glasses," *Ferroelectrics Letters Section*, vol. 38, no. 1-3, pp. 1-10, 2011.

[41] D. Umamaheswari, B. C. Jamalaiah, T. Sasikala, I. Kim, and L. R. Moorthy, "Photoluminescence properties of Sm^{3+} doped SFB glasses for efficient visible lasers," *Journal of Non-Crystalline Solids*, vol. 358, no. 4, pp. 782-787, 2012.

[42] V. Venkatramu, P. Babu, C. K. Jayasankar, T. Tröster, W. Sievers, and G. Wortmann, "Optical spectroscopy of Sm^{3+} ions in phosphate and fluorophosphate glasses," *Optical Materials*, vol. 29, no. 11, pp. 1429-1439, 2007.

[43] N. Wantana, S. Kaewjaeng, S. Kothan, H. J. Kim, and J. Kaewkhao, "Energy transfer from Gd^{3+} to Sm^{3+} and luminescence characteristics of CaO–Gd$_2$O$_3$–SiO$_2$–B$_2$O$_3$ scintillating glasses," *Journal of Luminescence,* vol. 181, pp. 382-386, 2017.

[44] T. Suhasini, J. S. Kumar, T. Sasikala, K. Jang, H. S. Lee, M. Jayasimhadri, J. H. Jeong, S. S. Yi, and L. R. Moorthy, "Absorption and fluorescence properties of Sm^{3+} ions in fluoride containing phosphate glasses," *Optical Materials,* vol. 31, no. 8, pp. 1167-1172, 2009.

[45] R. G. A. Kumar, S. Hata, K. Ikeda and K. G. Gopchandran, "Influence of metal ion concentration in the glycol mediated synthesis of Gd$_2$O$_3$:Eu^{3+} nanophosphor," *Ceramics International*, vol. 40, no. 2, pp. 2915-2926, 2014.

[46] G. Vimal, K. P. Mani, P. R. Biju, C. Joseph, N. V. Unnikrishnan, and M. A. Ittyachen, "Structural studies and luminescence properties of CeO$_2$:Eu^{3+} nanophosphors synthesized by oxalate precursor method," *Applied Nanoscience*, vol. 5, pp. 837-846, 2015.

[47] P. K. Kaiser, "Determination of CIE chromaticity coordinates of colored lights produced by a projection color mixer," *Behavior Research Methods & Instrumentation*, vol. 6, no. 5, pp. 473-476, 1974.